Supporting Information

Encapsulating $Bi_2Ti_2O_7$ (BTO) with Reduced Graphene Oxide (RGO): An Effective Strategy to Enhance Photocatalytic and Photoelectrocatalytic activity of BTO

Satyajit Gupta[1] and Vaidyanathan (Ravi) Subramanian [1]*

[1]*Department of Chemical and Materials Engineering, University of Nevada, Reno, NV 89557, USA.*

**corresponding Author E-mail: ravisv@unr.edu; Fax: +1 775-327-5059; Tel: +1 775-784-4686.*

Section 1. Synthesis of bismuth titanate (BTO)

(a) Preparation of stock solution

Titanium isopropoxide was hydrolyzed in water to form a white precipitate of titanium oxohydroxide/hydroxide. The precipitate was dissolved in concentrated nitric acid with ultrasonication followed by the addition of distilled water to maintain an acid concentration at 1M. This solution was used as a titanium precursor for the BTO synthesis. Bismuth nitrate stock solution of 0.1 M concentration was prepared by dissolving solid bismuth nitrate in nitric acid of 1 M concentration.

(b) Preparation of the oxide photocatalyst

In this study, the synthetic procedure is based on a co-precipitation of the respective salts followed by calcination in a furnace at 600°C (**Figure S1)**. Equal volumes (50 mL) of the titanium precursor and bismuth nitrate were added to a 250 mL beaker and stirred. Then, ~50 mL of strong ammonium hydroxide solution was added, which caused the formation of the precipitate of all dissolved metals in the form of hydroxides. The precipitate was collected by centrifugation and washed multiple times with deionized water to remove excess ammonium hydroxide. The gel-type precipitate was dried in an oven at~150°C for 2 h. The obtained dried mass was crushed into fine powder using a mortar-pestle and transferred to a small crucible. It was placed inside a larger crucible containing bismuth oxide which increases the outer Bi vapor pressure. The crucible was kept inside a furnace [Lindberg Bluebox furnace from Thermo Fisher Scientific]. The temperature of the furnace was increased from 25°C to 600°C in the first 2 h. The furnace was maintained for 4 h, at 600°C. After that, temperature was decreased to 25°C in 1 h.

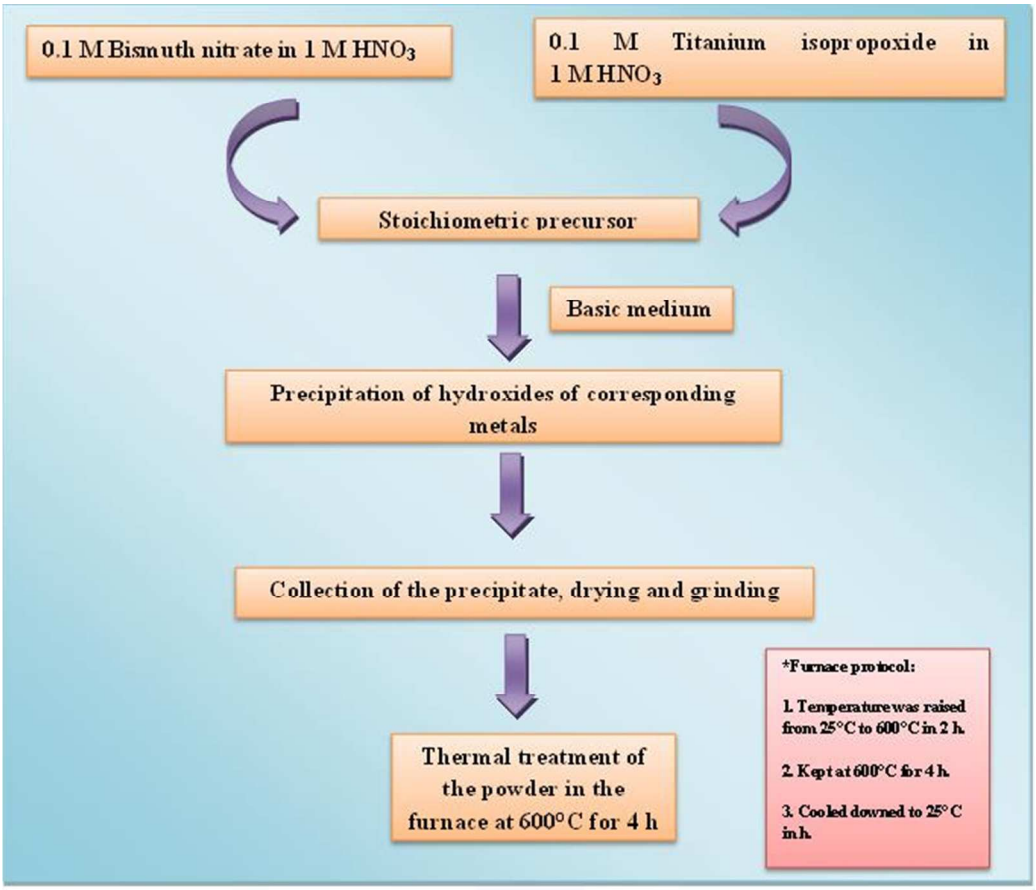

Figure S1. The scheme describes the step-by-step approach to the synthesis of BTO.

Section 2: Synthesis of graphene oxide (GO) by modified Hummer's method

In a typical synthetic procedure, graphite powder, $NaNO_3$, and concentrated H_2SO_4 were stirred together in an ice bath for 30 min. After that, $KMnO_4$ was slowly added to it resulting in the formation of a dark green color. The addition was carried out in a controlled manner so that temperature did not reach beyond 20°C. After this step, the ice bath was removed. At this point, the temperature of the solution was increased up to 40°C while keeping the reaction under stirring for 30 min. The mixture became a thick paste. D.I. water was slowly added to it. This reaction is exothermic and increases the temperature of the solution. The solution was further heated up to 95°C and maintained at this temperature for 30 min. Then, warm D.I water was added followed by slow addition of 30% H_2O_2 solution to reduce the excess $KMnO_4$. The color of the solution changed from dark brown to yellow. The mixture was stirred for some time and filtered out from the hot solvent. The obtained filtered cake was washed with warm water several times. Then the recovered cake was dispersed in water by sonication followed by centrifuge-aided separation. The separated mass was dried and preserved for further characterization and composite preparation.

Section 3 Electrode preparation with the powdered catalysts

The powdered samples of BTO and rGBTO were mixed thoroughly with terpenol in a mortar and pestle. They were coated on the conducting ITO coated glass slides (ITO coated glass plates were obtained from Pilkington Ford,OH). The ITO coated slides were heated at ~80°C and, annealed at 350°C for 4 h under an inert (N_2) atmosphere.

Section 4: Photocatalytic slurry reactor for the H_2 evolution

The slurry reactor (purchased from Ace Glass, Vineland, NJ) with a capacity of 500 mL was used to study hydrogen evolution. The reactor configuration and set-up is shown in **figure S2**. In a typical procedure, 0.15 g of catalyst was mixed with 250 mL water and 50 mL of methanol (as a sacrificial agent). In experiments involving other additives, formic acid or fomaldehyde were used in the same v/v ratio as methanol/water. The above solution was sufficiently purged with argon gas to remove the dissolved gas. The gas produced during the photocatalytic process was collected by downward displacement of water in a column. The gas composition was analyzed using a gas chromatograph (SRI GC model 8610C, Multi gas channel #3 with a TCD detector) at various time intervals.

Table 1. Medium pressure immersion type, quartz mercury vapor lamp was used for the photocatalytic reaction and the energy output of the light source is summarized in the following table.

Wavelength range (nm)	Energy output (Watt)	Energy output (%)
220-280 (Far UV)	27	15.4
280-320 (Middle UV)	28.7	16.3
320-400 (Near UV)	28	15.9
400-800 (Visible)	75.7	43.1
800-1400 (Infrared)	16.4	9.3
Total:	175.8	100

Figure S2. The photograph of the slurry reactor setup used for performing the hydrogen evolution reactions using aqueous mixtures and BTO/RGO photocatalysts with different ratios. (Details of the reactor setup can be found in Ref 26 of the main manuscript)

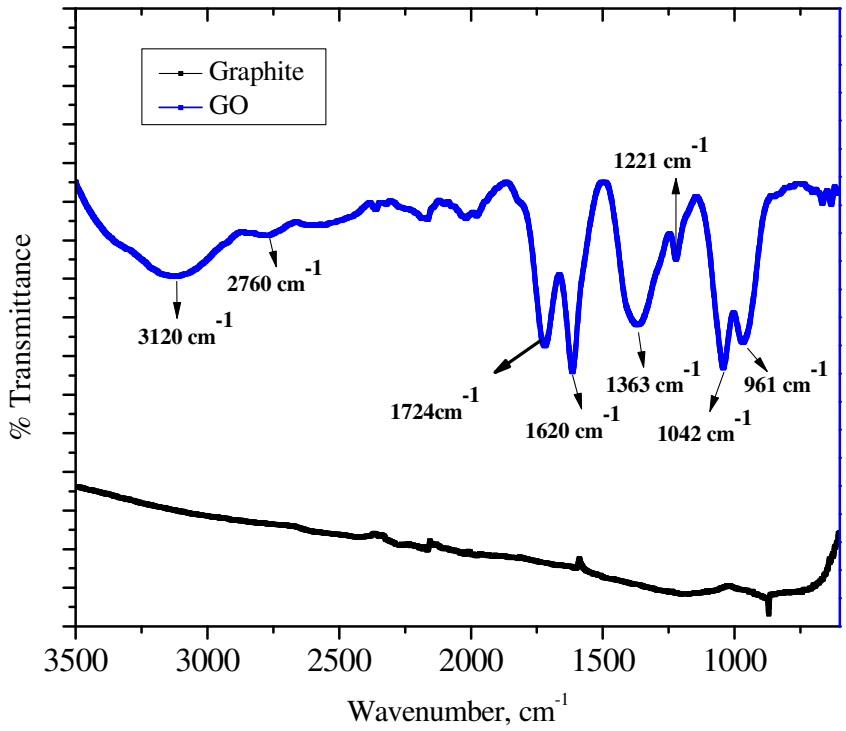

Figure S3. The FTIR spectra of the (top) GO and (bottom) neat graphite.

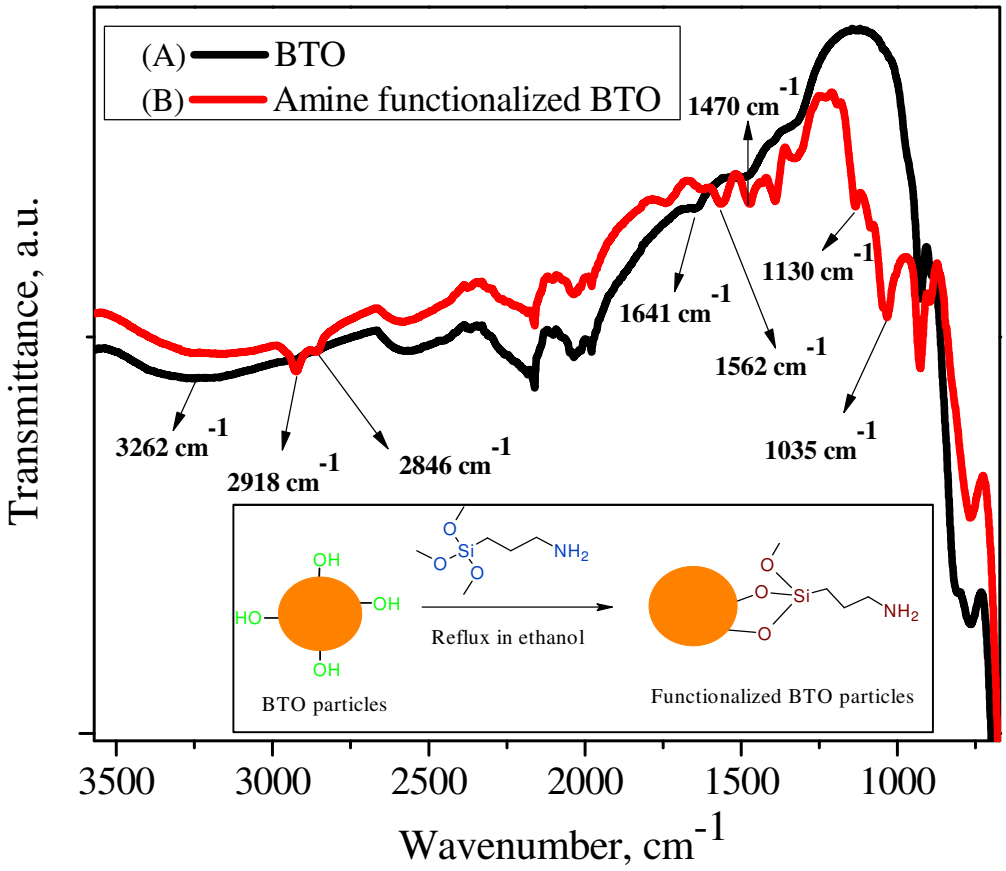

Figure S4. The Fourier transform infra-red spectra of (A) BTO and (B) amine functionalized BTO are shown. The relevant peaks are identified and discussed in detail in section 3.2. The inset shows the details of the chemistry involved during the amine functionalization of BTO.

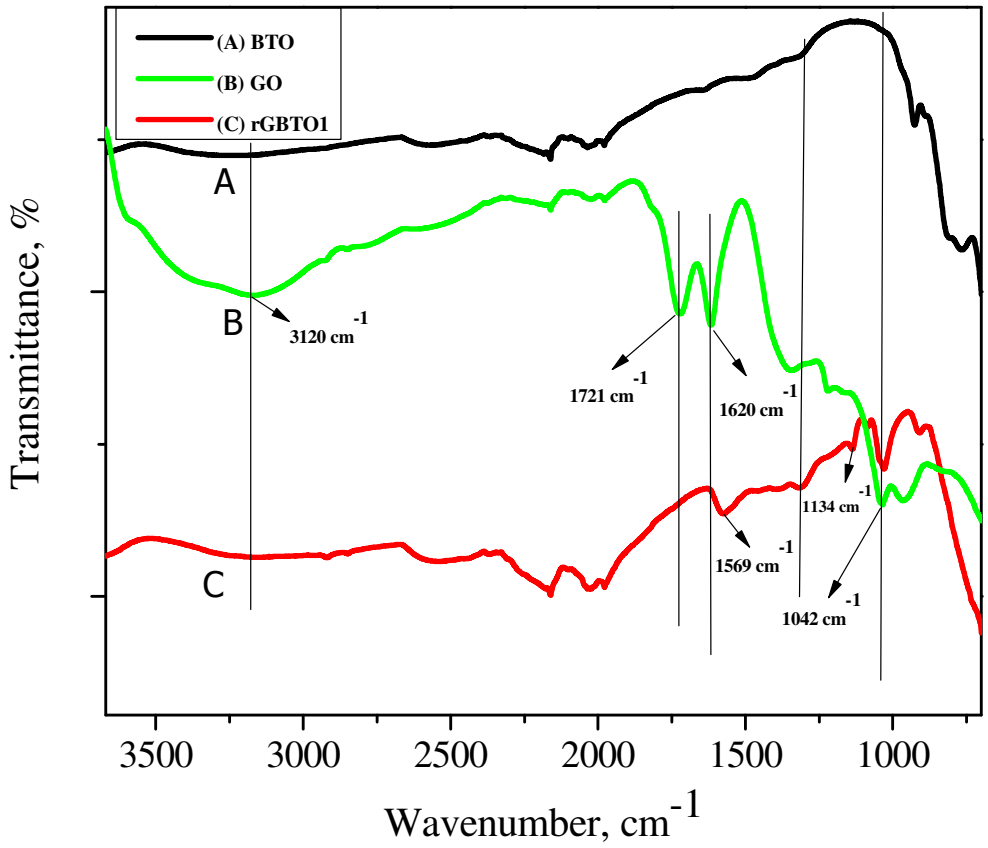

Figure S5. The Fourier transform infrared spectra of (A) BTO, (B) GO, and (C) rGBTO1 composite are shown.

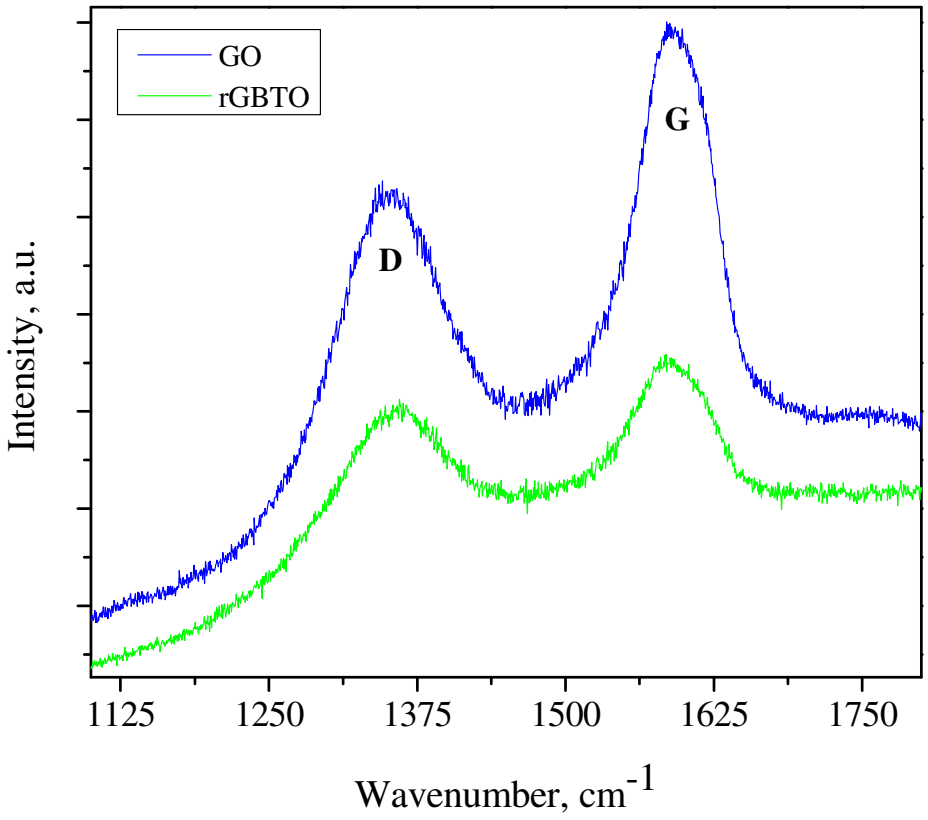

Figure S6. The Raman spectra of GO and the RGO encapsulated BTO (rGBTO).

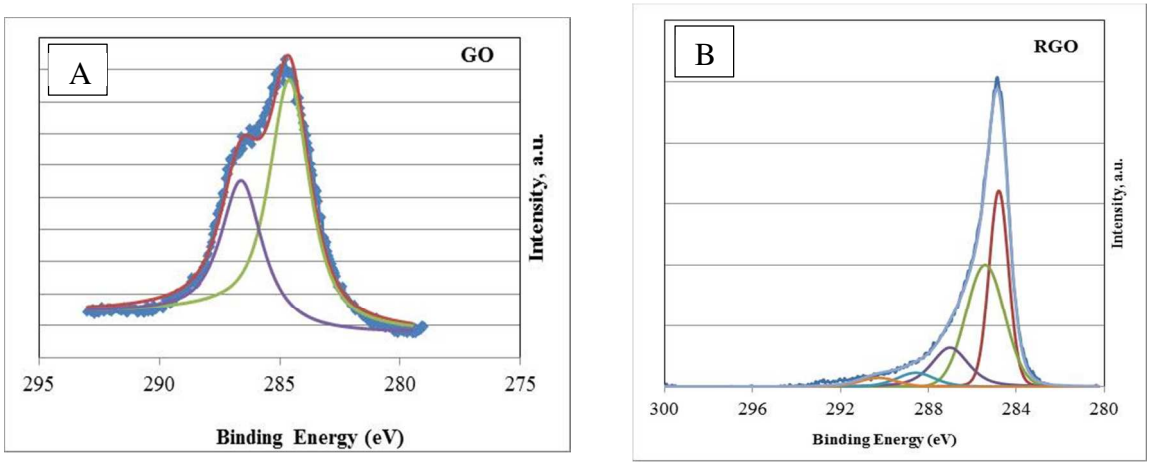

Figure S7. Deconvoluated XPS spectra of (A) C_{1S} of GO and (B) C_{1S} of RGO.

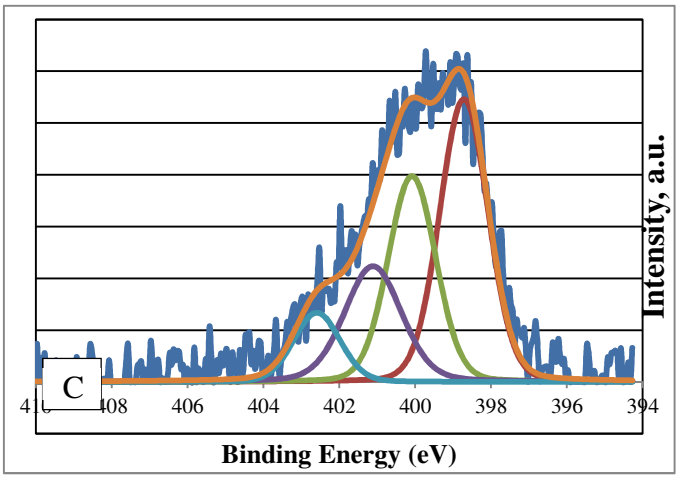

Figure S8. The XPS spectra of N_{1s} of RGO is shown. The deconvoluation of this peak demonstrates that, nitrogen exists in three different chemical forms, pyridinic (398.6 eV), pyrollic (400 eV) and graphitic/quaternary nitrogen (401 eV). A relatively low intensity peak found at ~403 eV could be due the formation of pyridine-N-oxide (N^{+}-O^{-}), due to surface oxidation.

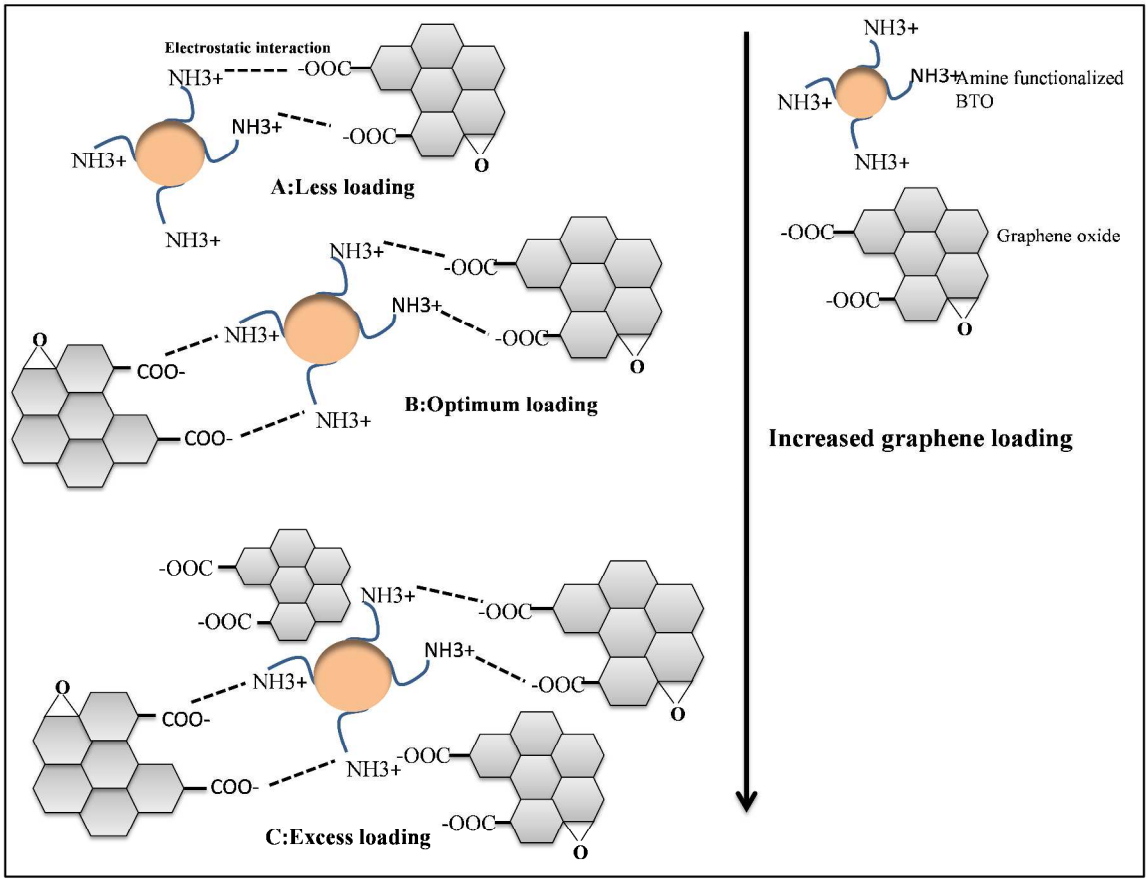

Figure S9. The schematic illustrates the surface processes that occur when the BTO: RGO ratio is changed. The chemical interactions during the electrostatic self-assembly are classified as three arbitrary domain (A) less loading of BTO, (B) optimal loading of BTO, and (C) Excess loading of BTO.

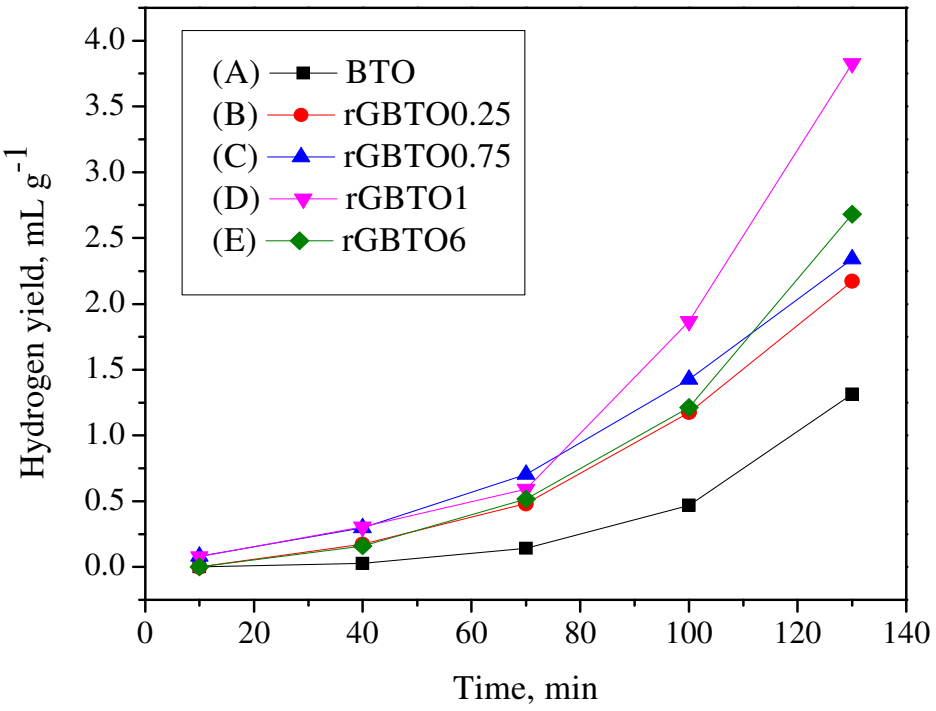

Figure S10. The time resolved hydrogen yield obtained using the (A) BTO and the (B-E) BTO/RGO composite catalysts with RGO content varied from 0.25 wt% to 6 wt%. The results presented in this time resolved graph are obtained in the presence of a water/methanol mixture with 250/50 (v/v) composition and UV-vis illumination continuously over a period of 130 minutes.

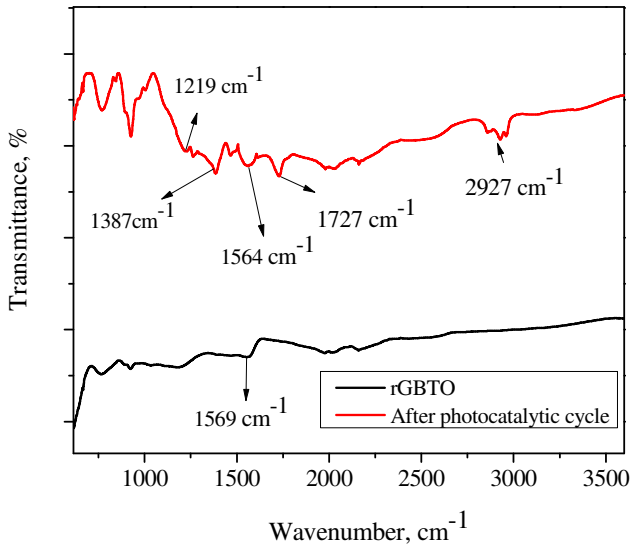

Figure S11. The FTIR analysis of the (rGBTO) photocatalyst after (top) being used in a photocatalysis experiment over a duration of 2.1 h. The catalyst was recovered, dried, and examined for the presence of surface functional groups. The pristine (unused) catalyst is shown as well (below).

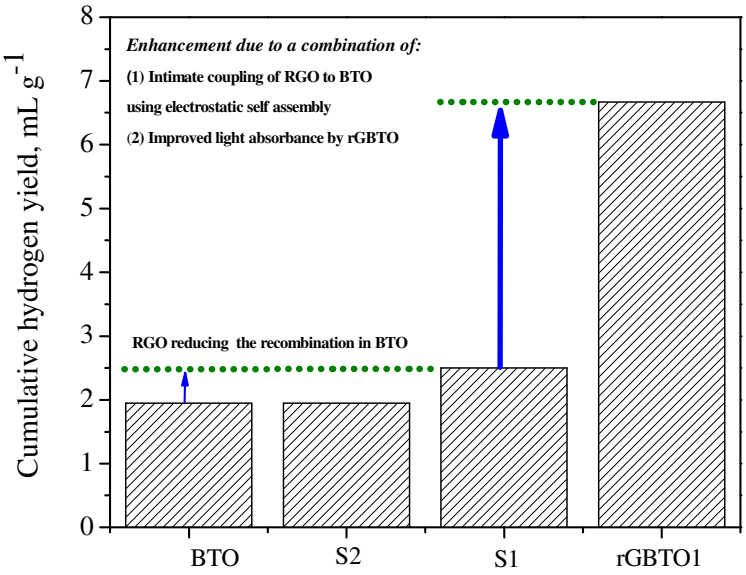

Figure S12. The comparison of the hydrogen yield obtained using the rGBTO1 (RGO = 1 wt %) with other controls. These controls include Pristine BTO, a physical mixture of BTO with RGO without functionalization (S1) and composite obtained using solid state mixing (S2).

Section 5: Photocatalytic hydrogen generation: Control experiments

Additional experiments utilizing RGO and RGO - BTO in different forms where performed as a control and contrasted with the rGBTO for hydrogen yield (Figure S12). No detectable amount of hydrogen was generated without BTO indicating that RGO alone is not capable of photocatalysis. Experiments were also performed using solution mixed GO and pristine BTO (non-functionalized) S1. This mixture showed a hydrogen yield similar to the BTO alone but significantly less hydrogen yield compared to the rGBTO1. A little improvement as compared to BTO could be due to the adsorbed fraction of RGO promoting some level of charge separation. However, the absence of close contact possible only due to electrostatic interaction is evident with this physical mixture. The result of this is an overall decrease in hydrogen yield as compared to self-assembled rGBTO1 structure.

Further a third control was also examined. The sample S2 was prepared as a physical mixture of the preformed RGO and BTO. S2 showed no improvement compared to BTO as well. This result is similar to the hydrogen yield using pristine BTO, primarily because solid state mixing also does not help in forming good interfacial contacts since reduced graphene oxide remain as a phase separated fraction. The analysis of the earlier sections indicates that the improvement in photocatalytic hydrogen yield is due to a combination of (1) intimate coupling between RGO and BTO and (2) improved light absorbance by the rGBTO composite nanostructures. Further study is needed to decouple these simultaneously occurring two contributions in the rGBTO composites.

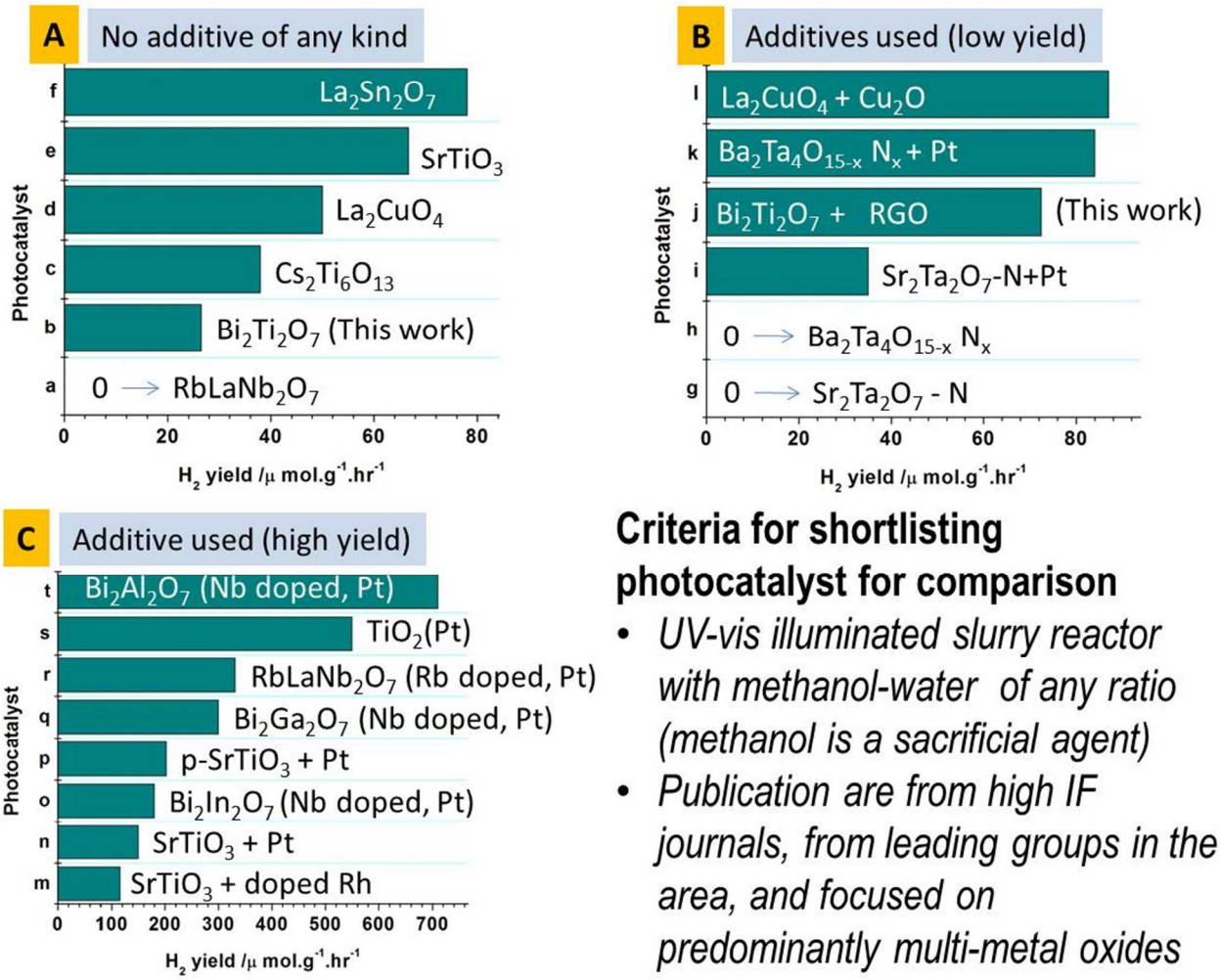

References:

[a,r] ***ACS Catal.*** 2013, 3, 2547–2555.[1]
[b,j] $Bi_2Ti_2O_7$: The present work.
[c] ***J. Mater. Chem.***, 1997, 7, 777–780.[2]
[d,l] ***Catal. Comm.*** 2013, 36, 20–24.[3]
[e,n] ***J. Catal.*** 1988, 111, 296-301.[4]
[f] ***J. Phys. Chem. C*** 2007, 111, 11879-11887.[5]
[g,h,i,k] ***J. Mater. Chem. A,*** 2013, 1, 5651–5659.[6]
[m] ***Chem. Eng. J.*** 2013, 223, 200–208.[7]
[o,q,s,t] ***Chem. Mater.*** 2001, 13, 1765-1769.[8]
[p] ***ACS App. Mater. Int.*** 2013, 5, 3683-3699.[9]

Figure S13. Comparison of the 'catalyst used in this work' with other benchmark catalysts in the similar class in terms of hydrogen evolution.

REFERENCES:

(1) Boltersdorf, J.; Maggard, P. A. Silver Exchange of Layered Metal Oxides and Their Photocatalytic Activities. *ACS Catal.* **2013**, *3*, 2547−2555.

(2) Kudo, A.; Kondo. T. Photoluminescent and Photocatalytic Properties of Layered Caesium Titanates, $Cs_2Ti_nO_{2n+1}$ (n=2, 5, 6). *J. Mater. Chem.*, **1997**, *7*, 777–780.

(3) Zhang, Z.; Chen, X.; Zhang, X.; Lin, H.; Lin, H.; Zhou, Y.; Wang. X. Synthesis of Cu_2O/La_2CuO_4 Nanocomposite as an Effective Heterostructure Photocatalyst for H_2 Production. *Catal. Comm.* **2013**, *36*, 20–24.

(4) Kudo, A.; Tanaka, A.; Domen, K.; Onishi, T. The Effects of the Calcination Temperature of $SrTiO_3$ Powder on Photocatalytic Activities. *J. Catal.* **1988**, *111*, 296-301.

(5) Zeng, J.; Wang, H.; Zhang, Y. C.; Zhu, M. K.; Yan. H. Hydrothermal Synthesis and Photocatalytic Properties of Pyrochlore $La_2Sn_2O_7$ Nanocubes. *J. Phys. Chem. C* **2007**, *111*, 11879-11887.

(6) Chen, S.; Yang, J.; Ding, C.; Li, R.; Jin, S.; Wang, D.; Han, H.; Zhang, F.; Li, C. Nitrogen-doped Layered Oxide $Sr_5Ta_4O_{15-x}N_x$ for Water Reduction and Oxidation Under Visible Light Irradiation. *J. Mater. Chem. A* **2013**, *1*, 5651–5659.

(7) Shen, P.; Lofaro, J. C. L.; Woerner, W. R.; White, M. G.; Su, D.; Orlov, A. Photocatalytic Activity of Hydrogen Evolution Over Rh Doped $SrTiO_3$ Prepared by Polymerizable Complex Method. *Chem. Eng. J.* **2013**, *223*, 200–208.

(8) Zou, Z.; Ye, J.; Arakawa, H. Substitution Effects of In^{3+} by Al^{3+} and Ga^{3+} on the Photocatalytic and Structural Properties of the Bi_2InNbO_7 Photocatalyst. *Chem. Mater.* **2001**, *13*, 1765-1769.

(9) Kuang, Q.; Yang, S. Template Synthesis of Single-Crystal-Like Porous $SrTiO_3$ Nanocube Assemblies and Their Enhanced Photocatalytic Hydrogen Evolution. *ACS Appl. Mater. Interfaces* **2013**, *5*, 3683-3699.